NATIONAL AERONAUTICS AND SPACE ADMINISTRATION

Technical Memorandum 33-540

Plume Backscatter Measurements Using Quartz Crystal Microbalances in JPL Molsink (Molecular Sink)

Wolfgang Simon

JET PROPULSION LABORATORY
CALIFORNIA INSTITUTE OF TECHNOLOGY
PASADENA, CALIFORNIA

May 15, 1972

NATIONAL AERONAUTICS AND SPACE ADMINISTRATION

Technical Memorandum 33-540

Plume Backscatter Measurements Using Quartz Crystal Microbalances in JPL Molsink (Molecular Sink)

Wolfgang Simon

JET PROPULSION LABORATORY
CALIFORNIA INSTITUTE OF TECHNOLOGY
PASADENA, CALIFORNIA

May 15, 1972

PREFACE

The work described in this report was performed by the Propulsion Division of the Jet Propulsion Laboratory.

ACKNOWLEDGMENT

The author wishes to acknowledge the contribution of Dr. Jose E. Chirivella in overseeing the actual tests, and that of James B. Stephens and Ralph E. Bartera, who were responsible for the successful operation of the Molsink and the quartz crystal microbalance systems.

CONTENTS

CONTENTS (contd)

FIGURES (contd)

ABSTRACT

Recent tests in the JPL Molsink facility have provided the first quantitative evidence of gas flows in the far upstream region of small nozzles with large boundary layer flow. Gas mass fluxes were measured using quartz crystal microbalances. Both nitrogen and carbon dioxide gases were used as test gases. Gas deposition rates on the order of 100 monolayers per minute were detected 13 inches upstream of the nozzle exit plane. It is significant to note that the crystals detected gases considerably beyond the inviscid Prandtl-Meyer turning angle. Tests are currently continuing using improved cryogenic quartz crystal systems and additional types of gases. The data from these tests will be essential in the formulation of scaling laws and analytical prediction methods for viscous plume behavior.

INTRODUCTION

The interaction of plumes with spacecraft components can cause problems in such diverse areas as flight mechanics, materials and structures, communications, and scientific experiments. The possible problems are aggravated if a large percentage of the plume is composed of nozzle boundary layer gases. Because these have a lower velocity than the nozzle core gases, they have a higher potential of expansion and will cause a back, or upstream flow, of the exhaust gases. Although analytical methods, such as the method of characteristics, are available to predict plume characteristics for nozzles with negligible boundary layers, no equivalent proven methods are available for those with large boundary layers. Because the latter type of nozzles are typical of those used aboard unmanned spacecraft today, an experimental and analytical program to predict the nature of these plumes has been undertaken. The program has been described and some initial results have been reported in Reference 1. Recent tests using nitrogen and carbon dioxide gas have resulted in the first data on the amount of gas in the backflow region. Tests are continuing and the data reported in this TM, correlated with that now being generated, will result in the formulation of scaling laws and analytical techniques which will predict the distribution of gases in viscous plumes.

FACILITY AND TEST APPARATUS

Facility Characteristics

The Molsink is an ultra-high vacuum facility which consists of three concentric chambers. The innermost chamber is a sphere approximately 3.05 m (10 ft) in diameter, maintained at a temperature between 15 and 20 °K with gaseous helium. The walls are wedge-shaped, resembling an anechoic chamber, with a total surface area of approximately 186 m^2 (2000 ft^2). The chamber walls are also coated with titanium, which acts as "getter" material to trap helium and hydrogen that are not cryopumped by the 15°K surfaces. The facility is described in more detail in References 2, 3, and 4. A cross section of the Molsink is shown in Figure 1.

Quartz Crystal Microbalances (QCM)

Quartz Crystal Microbalances were positioned at various locations along the Molsink walls and used as gas detection devices. The QCM measures the mass per unit area adsorbed or desorbed on a piezoelectric quartz crystal surface through a change in the resonant frequency of the crystal. For a given crystal cut angle, there is a range of temperature for which the frequency change depends linearly on the rate of mass deposition. The QCM systems were orientated with their sensing surfaces perpendicular to a radial line drawn from the nozzle lip. Each QCM system included four crystal sensing surfaces, 1.3 cm in diameter, with their centers approximately 1.6 cm apart. Figure 2 is a photograph of the QCM system sensing heads as installed in the Molsink.

The QCM systems are driven by oscillators. Not all of the installed systems operated satisfactorily because of crystal/oscillator coupling problems. To condense and trap nearly all of the impinging gas the crystal surfaces must be maintained at low temperatures. The temperatures required to condense various gases are indicated in Table 1, which is taken from Reference 5. For example, to trap nitrogen at a pressure of 1.33×10^{-3} N/m^2 (10^{-5} torr), the crystal temperature must be below 29°K. Not all of the crystals were cooled to temperatures low enough to condense nitrogen.

The experience gained in these tests has been used to design and construct improved QCM systems which are operating successfully at low (< 29 °K) temperatures during present tests. The relative location of the test nozzle and the QCM systems from which data was obtained is shown in Figure 3.

TEST RESULTS

Tests were conducted with both nitrogen and carbon dioxide. The gas was released into the Molsink through a conical nozzle while the frequencies of the quartz crystals were recorded approximately every 30 seconds. The frequencies of the quartz crystals were also recorded when no gas was flowing in order to determine the mass of gas, previously deposited, leaving the crystal surface.

Test data was obtained for carbon dioxide gas at two locations, 0.33 m (13 in.) upstream of the exit plane (163 deg from the nozzle axis) and near the exit plane approximately 0.76 m (30 in.) from the nozzle. Because the crystal sensing surface of the QCM system upstream from the nozzle was not cold enough to condense the nitrogen, data for N_2 was obtained only near the exit plane.

The test results, in terms of change of mass on the sensing crystal surfaces, as a function of time are shown in Figures 4, 5, and 6 and are tabulated in Table 2. Figures 7 and 8 show the change of mass on the crystal as indicated by the QCM system during the gas off portion of the test and confirm the fact that the only significant change in frequency occurred during the time that gas was actually flowing through the nozzle. This verified the fact that desorption of the condensed gases from the crystal surfaces, during the test, was negligible.

Test results also indicate that the amount of gas found in the backflow region is strongly related to the proportion of the total nozzle gases in the boundary layer. In isentropic flow, the mass flux at a fixed location in the plume, can be assumed to be directly proportional to the nozzle plenum pressure. The test data, however, indicates that for a ratio of plenum pressures of 4.5:1, the mass flux ratio in the backscatter region is only 2.3:1. An integration of the experimentally determined Mach number profile at the exit plane of the nozzle shows that for a plenum pressure of 2.76×10^4 N/m^2 (4 psia) the boundary layer flow is approximately 32 percentage of the total mass flow, while at a pressure of 1.24×10^5 N/m^2 (18 psia) it is only 16 percent of the flow. Therefore, it would seem that the quantity of gas in the backscatter region is not directly proportional to the nozzle total mass flow and that the reduction in the boundary layer at the

higher plenum pressures and Reynolds numbers results in a smaller percentage of the nozzle total gas flow expanding into the backflow region.

DATA ANALYSIS

Data Reduction Procedure

The raw data in the form of quartz crystal frequencies is converted to mass per unit area changes on the crystal surface by means of the following theoretical formula:

$$\Delta m = \frac{4.35 \times 10^{-7}}{F^2} (\Delta F)$$

Δm = change in mass flux, gm/cm^2

F = resonant frequency of crystal, MHz

ΔF = change in frequency, Hz

The key assumption in the above formula is that the temperature of the crystal remains unchanged. The temperature sensitivity is a function of the angle at which the crystal is cut, and the crystals used in the QCM systems from which data was obtained are relatively insensitive to temperature changes. Therefore, it was not necessary to make temperature corrections.

Nozzle Characteristics

The flow characteristics of the nozzle used to generate the plume were measured during tests in the JPL space simulator. The nozzle is conical, with a 60:1 area ratio and 15° wall half angle. The percentage of the exit area occupied by the boundary layer increases rapidly with decreasing chamber pressure, as determined experimentally and indicated in Figure 9. It is clearly evident that viscous effects cannot be neglected in predicting the plume gas distribution.

Plume Maps

Inviscid plume gas distributions can be calculated quite accurately using the method-of-characteristics (MOC) which is valid for supersonic flow. The plume maps shown in Figures 10 and 11 were calculated for nitrogen and carbon dioxide. Also indicated on the figures is the Prandtl-Meyer turning angle based upon the nozzle exit Mach number, as calculated by the

MOC program. This is the maximum theoretical turning angle for the flow (or the angle at which the calculated density is zero) from this nozzle neglecting boundary layer effects.

The mass flux data from the quartz crystals can be translated into density if it is assumed that in the region of the quartz crystals the molecules have reached their maximum velocity (the velocity at which the total enthalpy has been completely converted to kinetic energy). The experimental data, thus converted, has also been plotted in Figures 10 and 11.

In Figures 12 and 13 the mass flux data is presented directly, thereby eliminating any error that may be due to deviations from adiabatic conditions which were assumed in converting the mass flux data to equivalent densities in Figures 10 and 11. The inviscid plume data shown is non-dimensionalized and indicates the mass flux off the centerline as a function of the centerline mass flux in the plume far field where the QCM systems are located.

The juxtaposition of the experimental data and the analytically derived inviscid plume data, in Figures 10, 11, 12 and 13, emphasizes the significant errors that can occur in plume behavior predictions when viscosity effects are neglected. The flow indicated by the QCM system, even though small, represents a significant percentage of the nozzle exhaust gases. A conservative calculation, assuming the average mass flux detected by the QCM systems is constant everywhere in the backflow region, at equal distances from the nozzle exit, shows that this flux represents 1.5% of the nozzle total mass flow in case of the carbon dioxide tests. For purposes of the calculation, the backflow region was defined to be the region upstream of the Prandtl-Meyer turning angle.

CONCLUSIONS

The significance of these tests is that they offer the first data of the amount of gas in the far upstream, or backflow, region of small nozzles. Despite the fact that this initial data is too limited to allow the formulation of accurate scaling laws, a number of conclusions can be made:

(1) The amount of gas in the region outside the Prandtl-Meyer angle is large enough to affect sensitive coatings on spacecraft instrumentation. In terms of monolayers, for example, the amount of carbon dioxide gas deposited on the #1 QCM system was on the order of 100 monolayers per minute. The small amount of gas required to coat a surface with several monolayers can be seen by referring to Table 3 which is a tabulation of the molecular properties of several gases from References 6 and 7. The mean free path of a molecule is proportional to the absolute temperature and inversely proportional to the pressure. Table 3, which also lists the free mean path of the test gases, indicates that the Knudsen number (based on the sensing element diameter of approximately 1.3 cm) in the vicinity of the QCM systems is large enough for free molecular flow conditions to exist.

(2) The proportion of the nozzle gases in the backflow region is a strong function of the nozzle boundary layer thickness. An increase in the nozzle gas flow of 4.5 coupled with a decrease in the percent of gases in the boundary layer of 50% resulted in an increase of 2.3 in the gases in the backflow region. The amount of gas in the backscatter region can therefore be reduced by nozzles, which by the nature of their design, inhibit the growth of boundary layers. This is one of the items being studied in an analytical effort paralleling the present experimental work and whose primary objective is to analytically predict the properties of viscous plumes.

(3) Finally, it can be stated that these tests have provided initial data which will help the formulation of analytical techniques required to accurately predict the characteristics of

viscous plumes. This is necessary to insure the compatibility of the spacecraft, its propulsion system, and its science package so that the mission objectives are not inadvertently compromised.

REFERENCES

1. Simon, W., "Nozzle Exhaust Plume Backscatter Experiment Using the JPL Molsink Facility," JPL Quarterly Technical Review, Vol. 1, No. 4, January 1972.

2. Stephens, J. B., "Spacecraft Mechanism Testing in the Molsink Facility," Proceedings of the 4th Aerospace Mechanisms Symposium, Technical Memorandum 33-425. Jet Propulsion Laboratory, Pasadena, Calif., Jan. 15, 1970.

3. Stephens, J. B., "Molecular Sink," Research/Development, July 1967.

4. Stephens, J. B., "Space Molecular Sink Simulator Facility Design," Spacecraft Rockets, June 1966.

5. Honig, R. E., Hook, H. O., RCA Review 21, 360 (1960).

6. Guthrie, A., Wakerling, R. K., Vacuum Equipment and Techniques, McGraw Hill, 1949.

7. Dushman, Saul, Scientific Foundations of Vacuum Technique, John Wiley & Sons, 1949.

Table 1. Temperature vs pressure for some common gases*

Pressure		Temperatures (°K) for vapor pressures				
N/m^2	torr	CO_2	N_2	H_2	NH_3	He_2
1.33×10^{5}	10^{3}					4.518
1.33×10^{1}	10^{-1}					0.980
1.33×10^{-2}	10^{-4}	98.1	31.4	5.38	116.5	
1.33×10^{-3}	10^{-5}	91.5	29.0	4.84	108.5	
1.33×10^{-4}	10^{-6}	85.7	27.0	4.40	102.0	
1.33×10^{-5}	10^{-7}	80.6	25.2	4.03	95.9	
1.33×10^{-6}	10^{-8}	76.1	23.7	3.71	90.6	

*From R. E. Honig and H. O. Hook RCA Review 21, 360 (1960)

Table 2. Rate of mass deposition of CO_2 and N_2 plume gases

Gas[1]	CO_2	CO_2	N_2	N_2
Nozzle Plenum Pressure, N/m^2 (psia)	2.8×10^4 (4)	2.8×10^4 (4)	2.8×10^4 (4)	1.2×10^5 (18)
Quartz Crystal Location[2]	#1	#2	#2	#2
Mass Flux, $kg/m^2 - s$	1.1×10^{-6}	2.7×10^{-6}	1.1×10^{-6}	2.5×10^{-6}

Note:

[1] Gas injected through 15° conical nozzle with 60:1 area ratio and a throat diameter of 2.54×10^{-3} m (0.100 in.).

[2] Quartz Crystal location shown in Figure 2.

#1 Approximately 0.33 m (13 in.) upstream of exit plane.

#2 Approximately at exit plane and 0.76 m (30 in.) from nozzle centerline.

Table 3. Molecular properties of gases

		CO_2	N_2	H_2
1.	Mass of molecule, 10^{-24} g	73	46.5	3.35
2.	Number of molecules per cm^2 in a monolayer, 10^{14}	5.34	8.10	15.22
3.	Mean free path at 15°C and 0.133 N/m^2 (1 μ Hg), cm	3.18	4.77	8.97
4.	Mass of monolayer per cm^2, 10^{-8} g	3.9	3.8	0.5

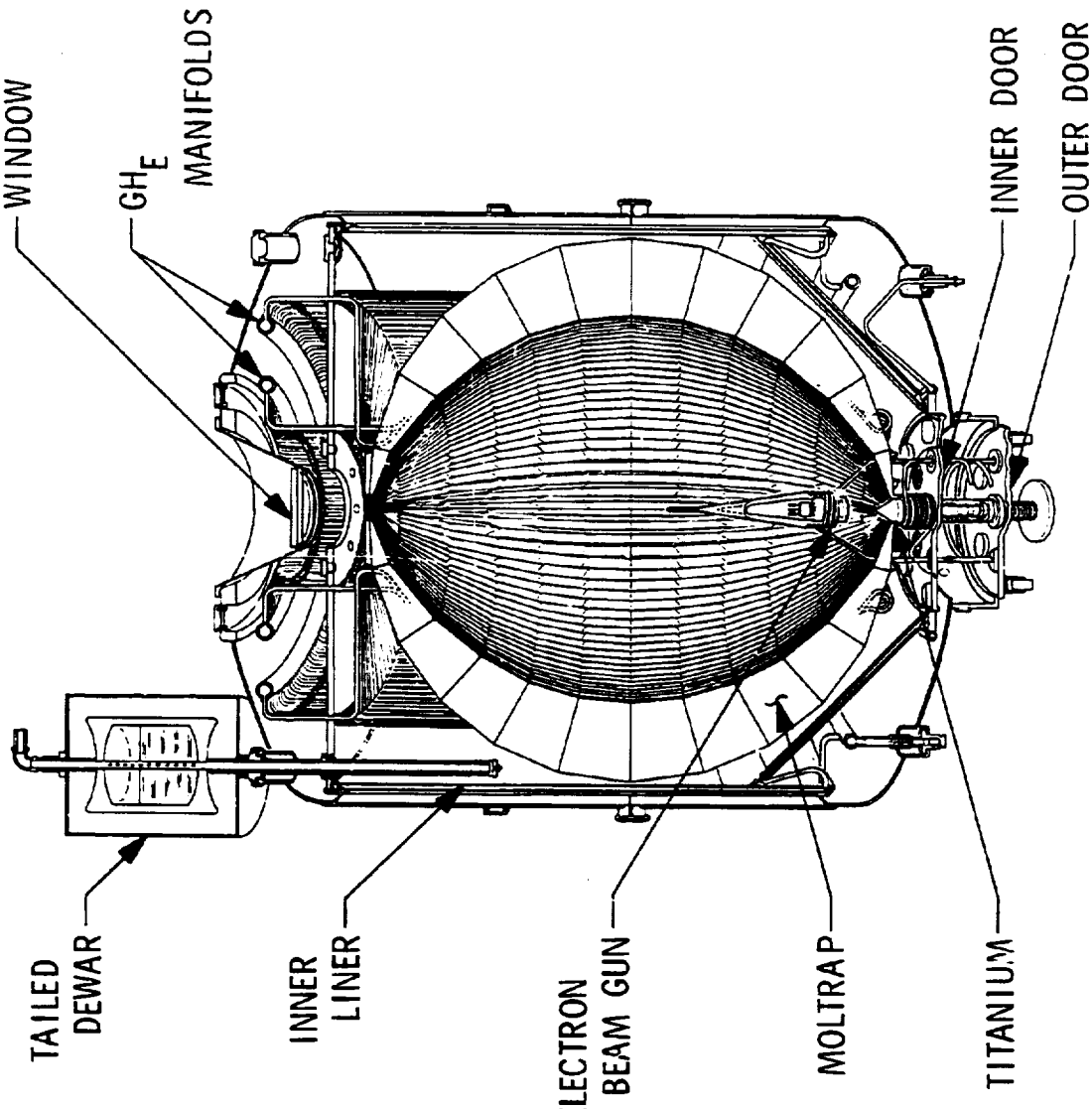

Fig. 1. Molsink Chamber

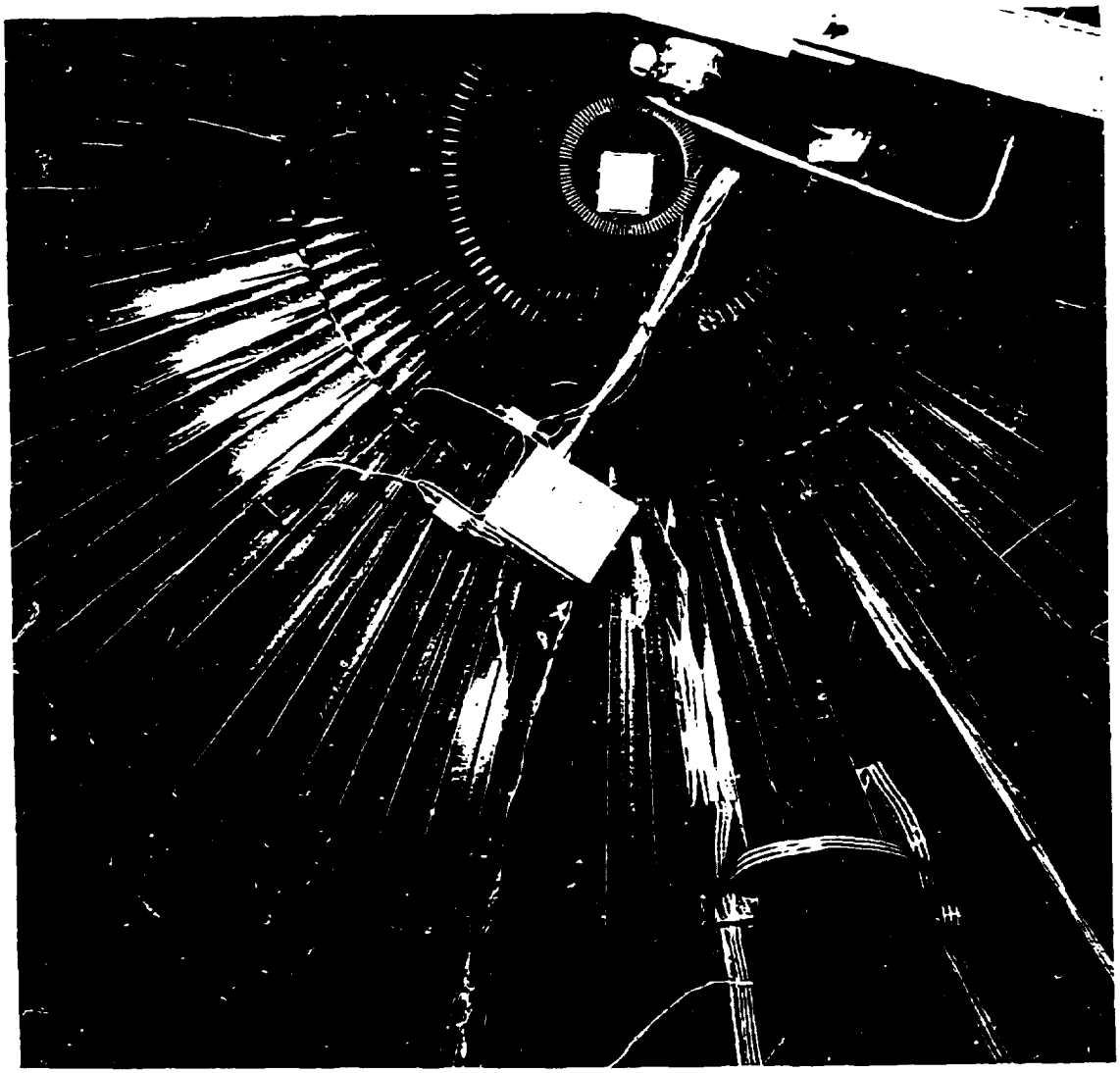

Fig. 2. QCM System Sensing Heads, as Installed in the Molsink

QCM SYSTEM 1, A = 10.2 cm
B = 33.0 cm
QCM SYSTEM 2, C = 10.2 cm
D = 76.2 cm

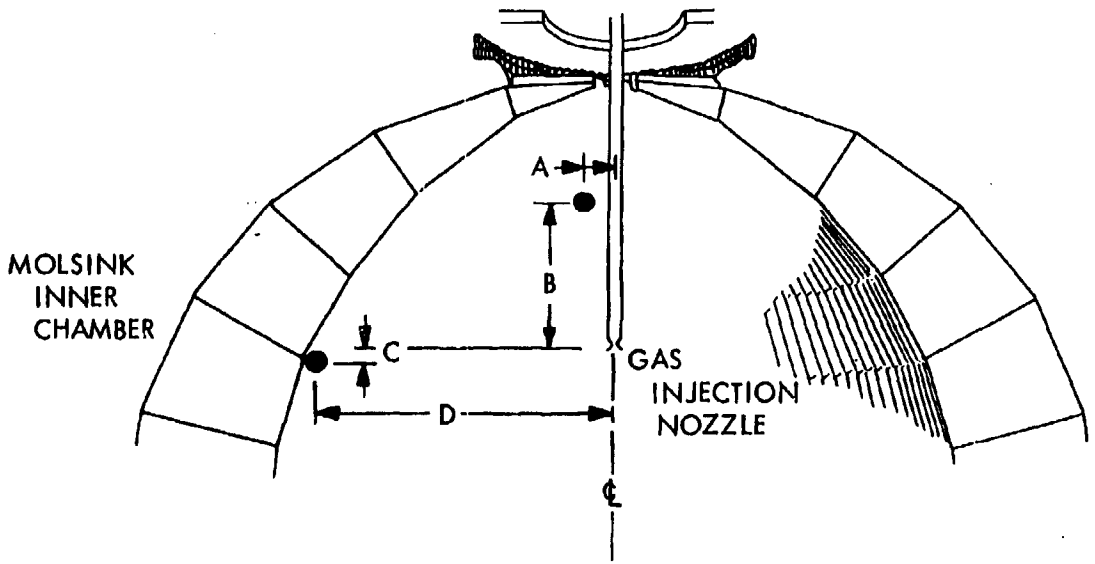

Fig. 3. Relative Location of QCM System and Test Nozzle

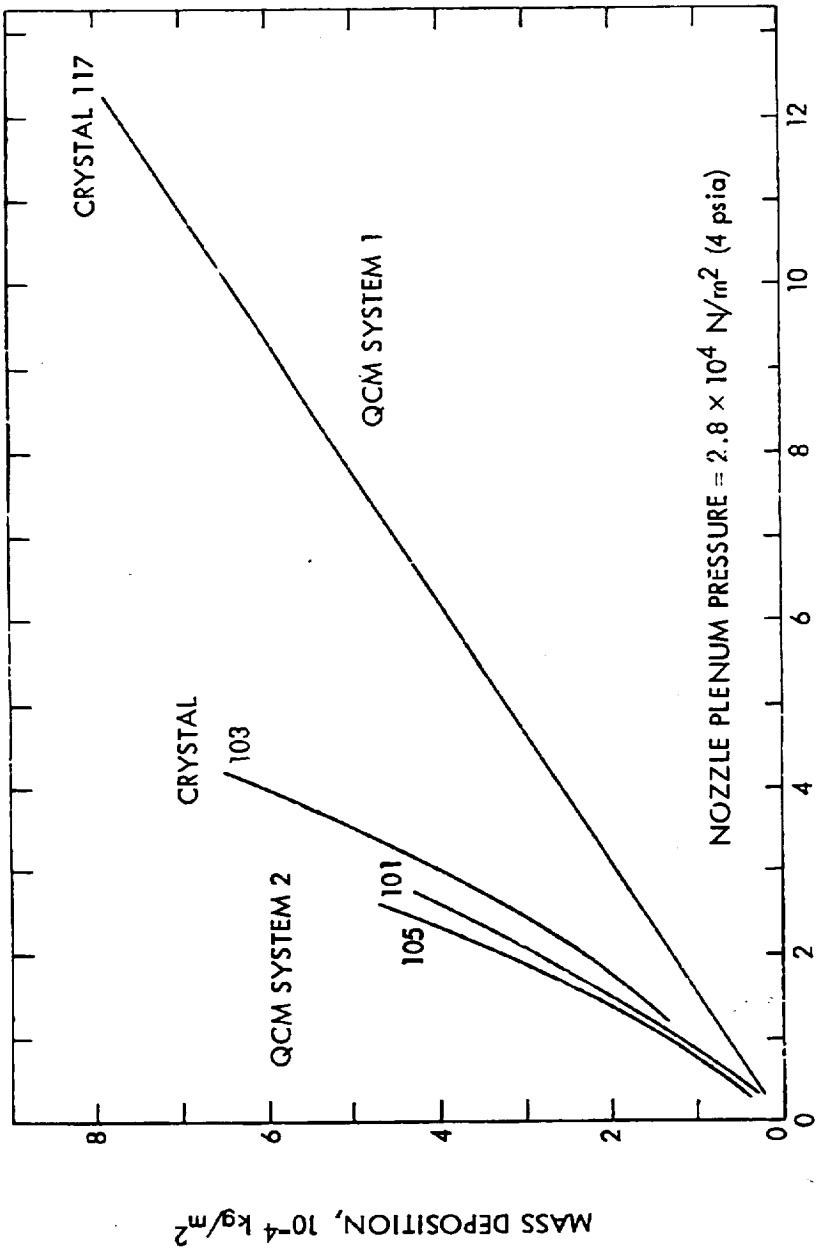

Fig. 4. Quartz Crystal Mass Deposition--CO_2

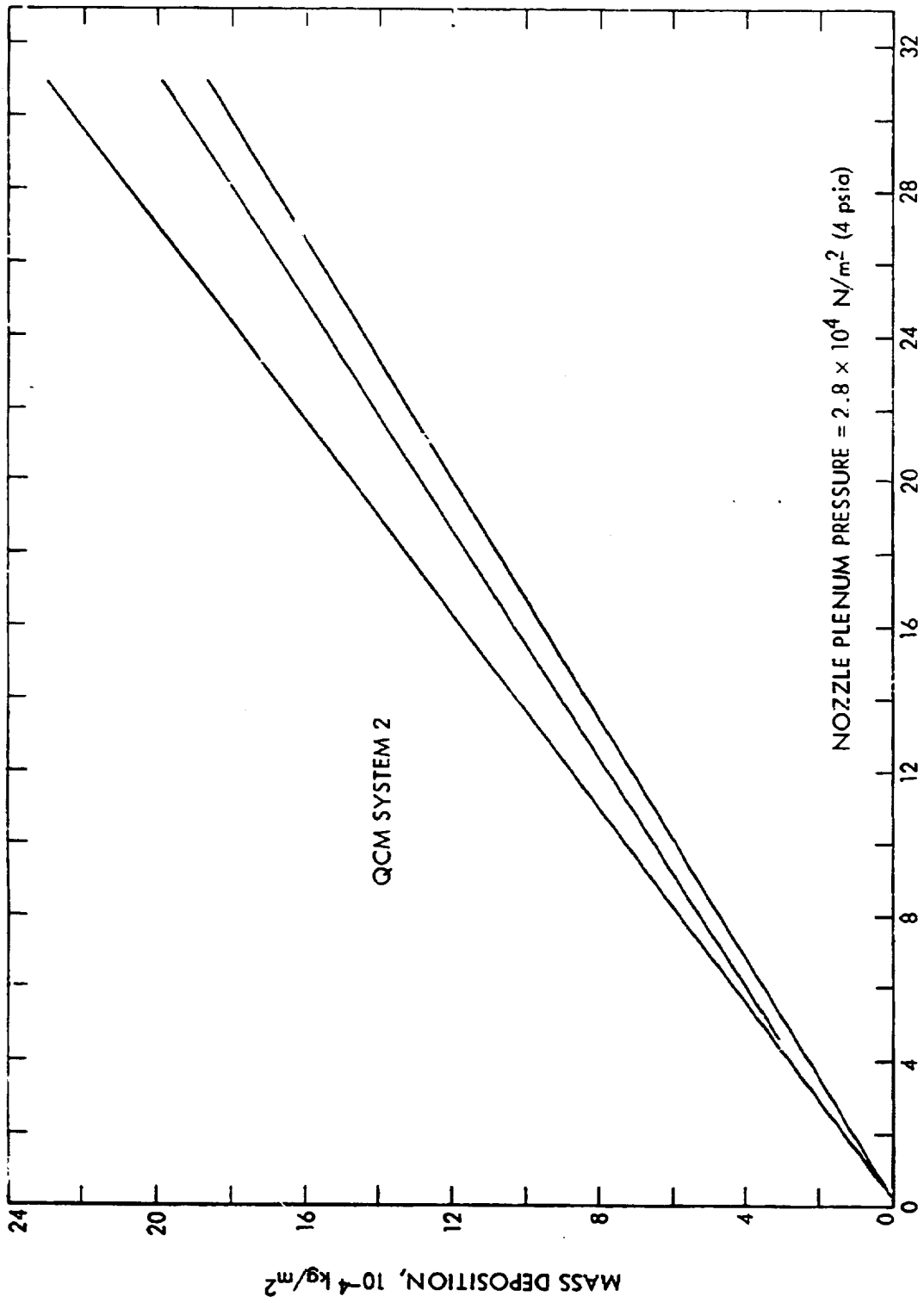

Fig. 5. Quartz Crystal Mass Deposition--N_2 at 2.8×10^4 N/m^2

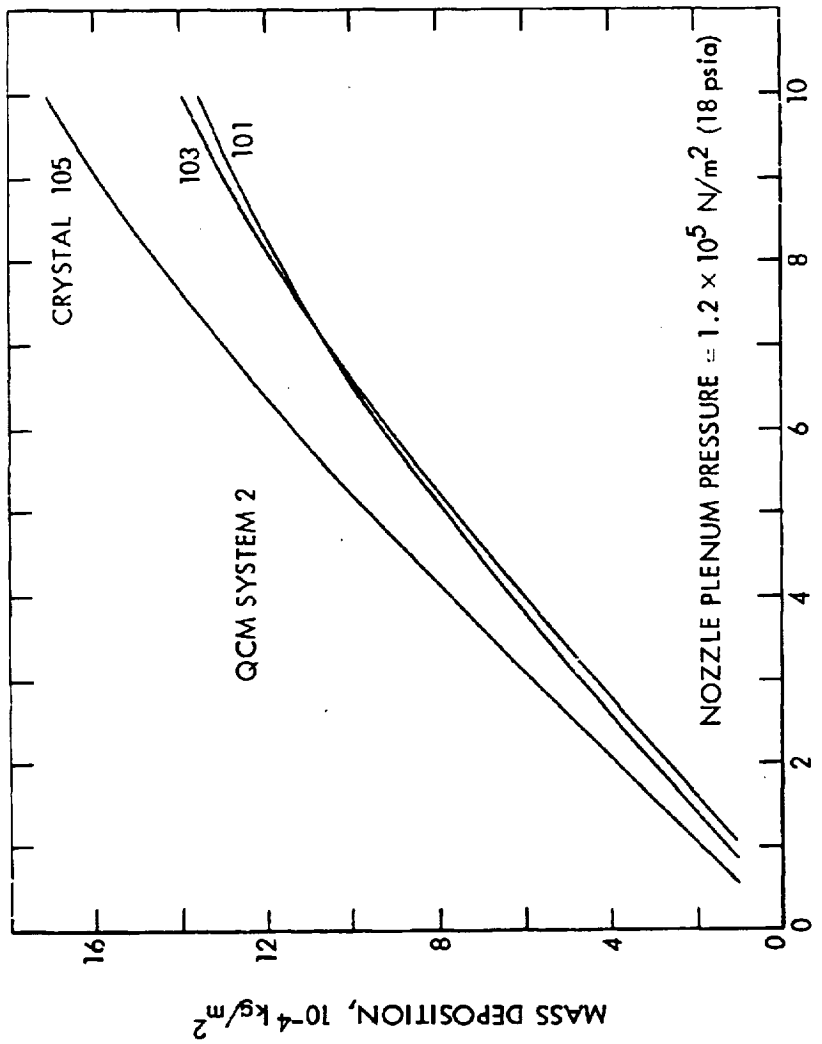

Fig. 6. Quartz Crystal Mass Deposition--N_2 at 1.2×10^5 N/m^2

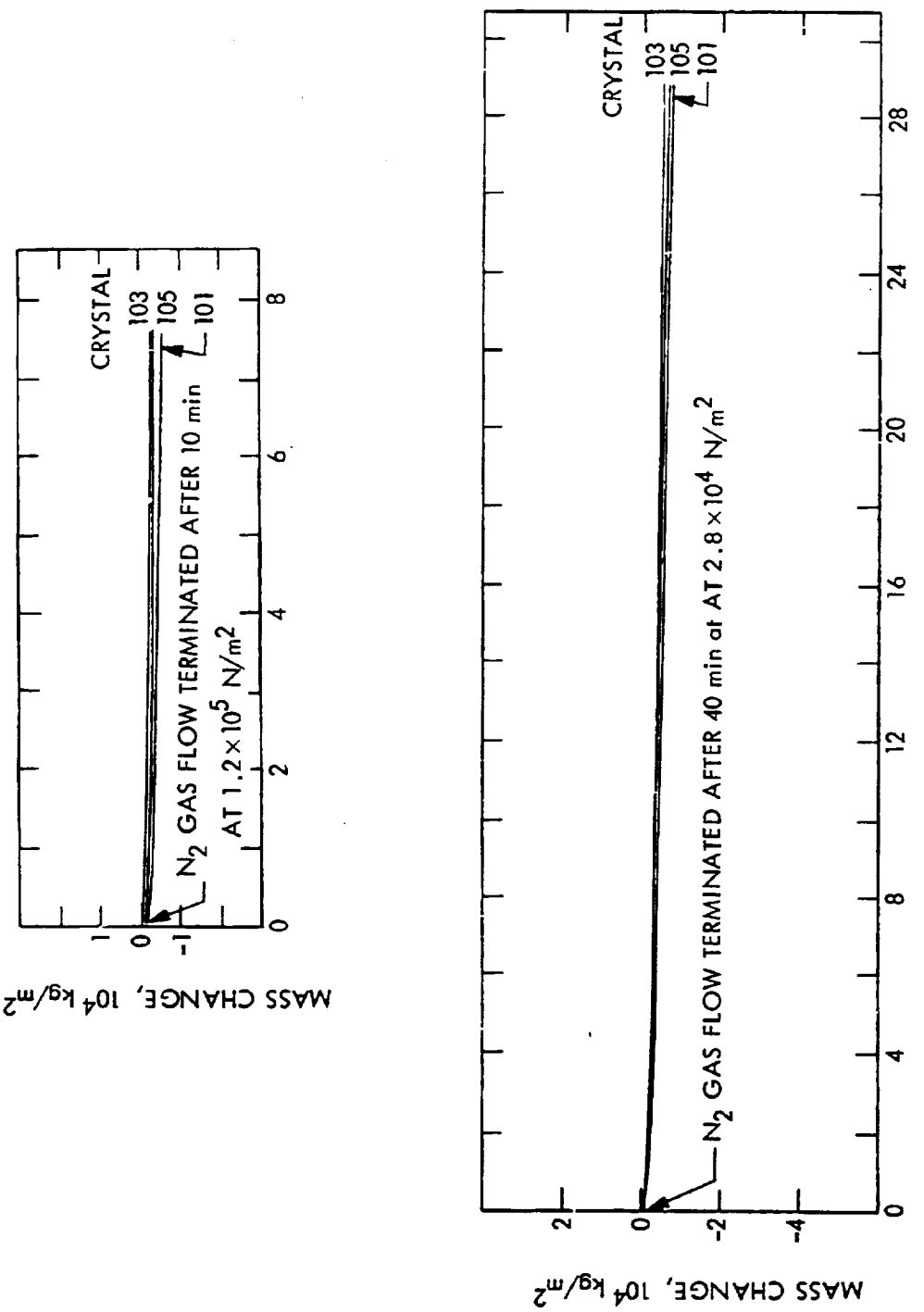

Fig. 7. Quartz Crystal Mass Deposition--No Gas Injection After N_2 Flow Terminated

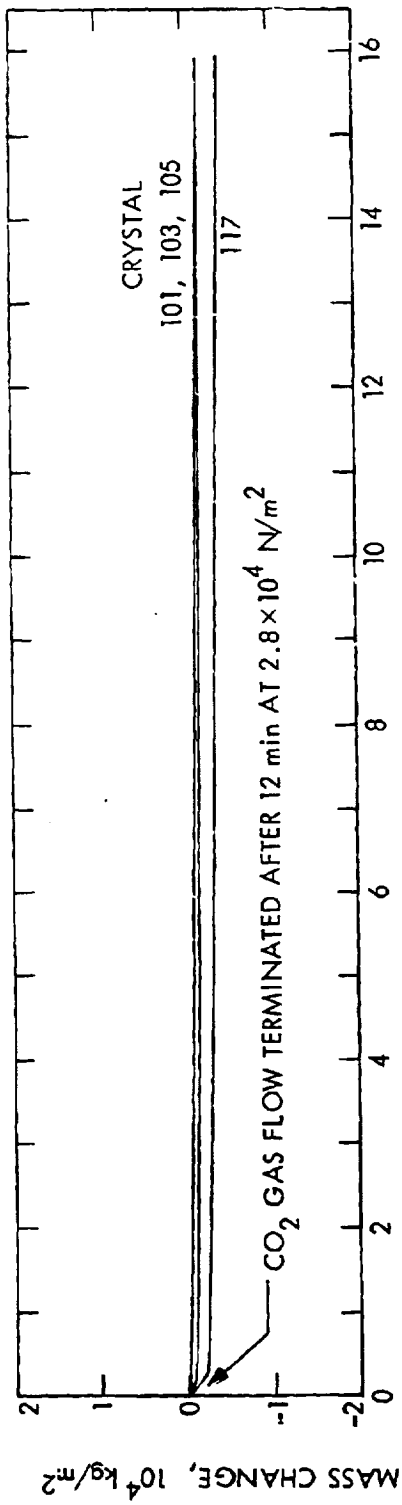

Fig. 8. Quartz Crystal Mass Deposition--No Gas Injection After CO_2 Flow Terminated

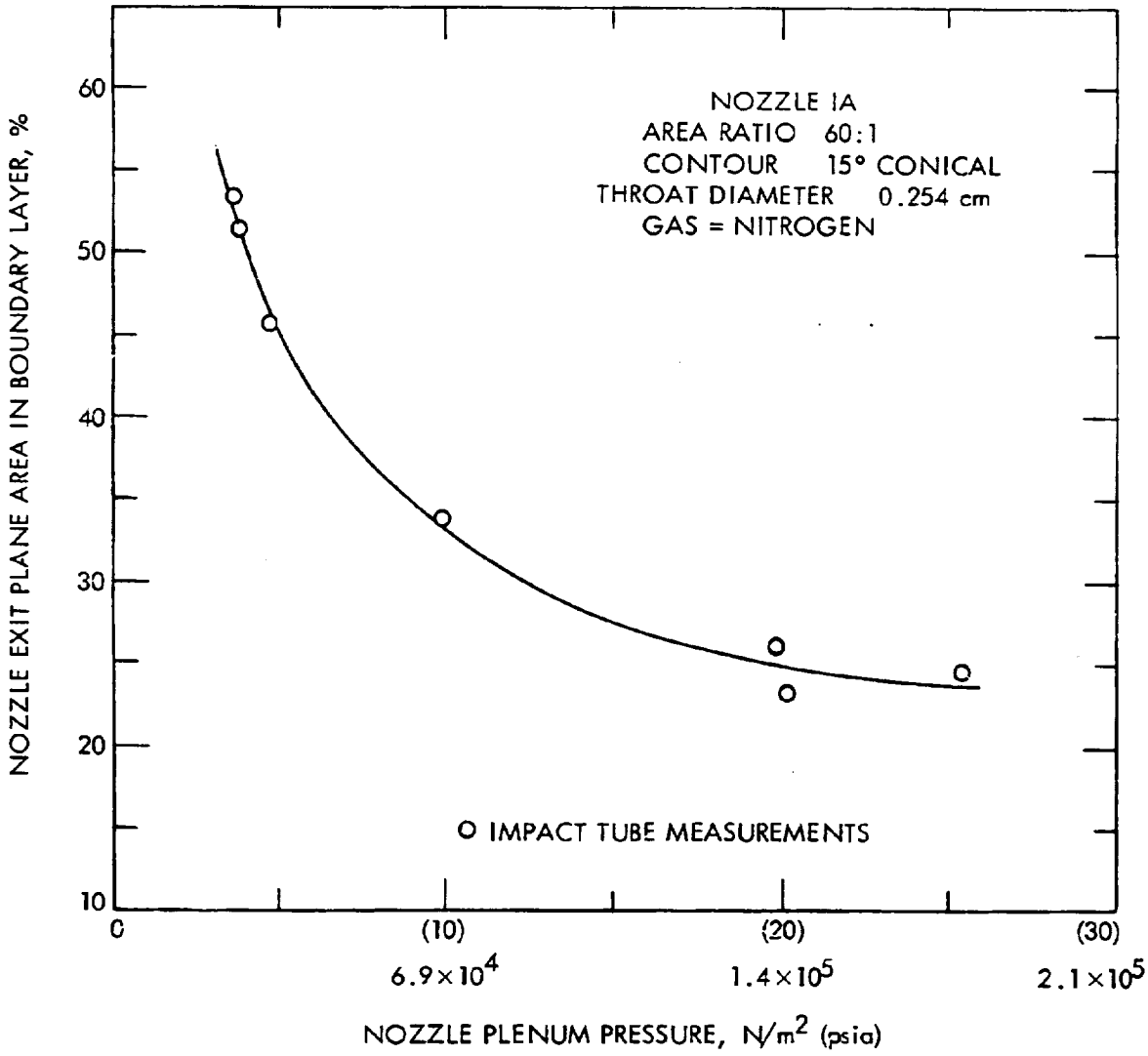

Fig. 9. Nozzle Boundary Layer Growth

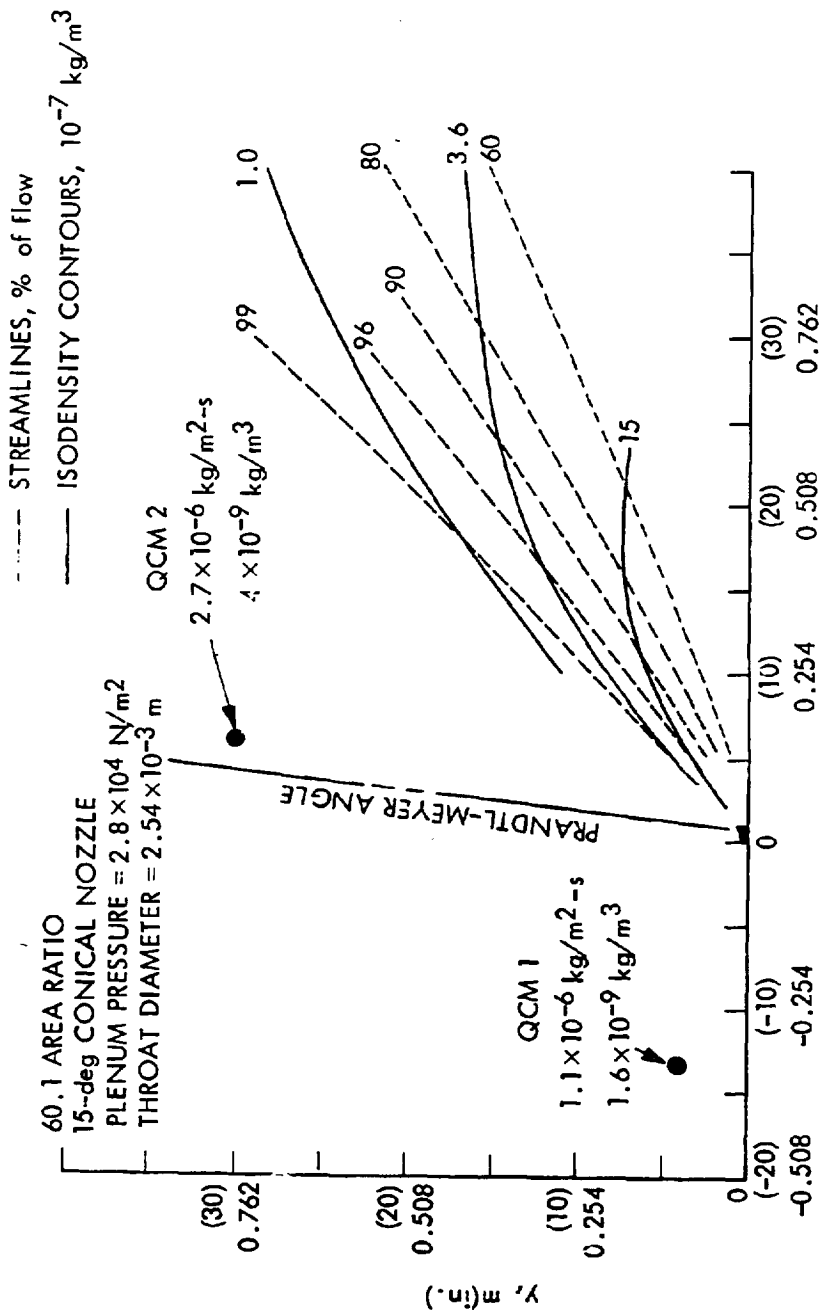

Fig. 10. Carbon Dioxide Plume Map

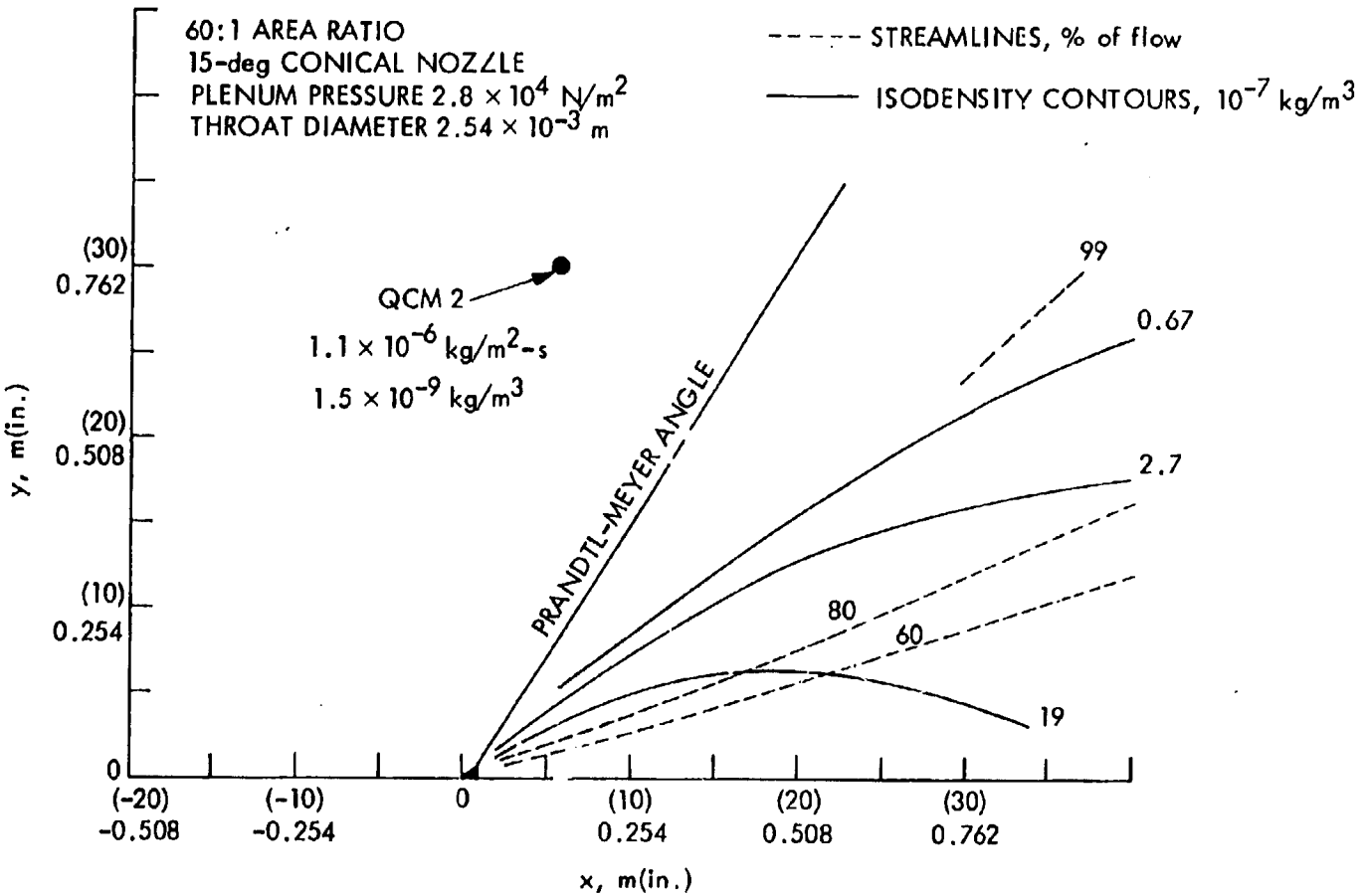

Fig. 11. Nitrogen Plume Map

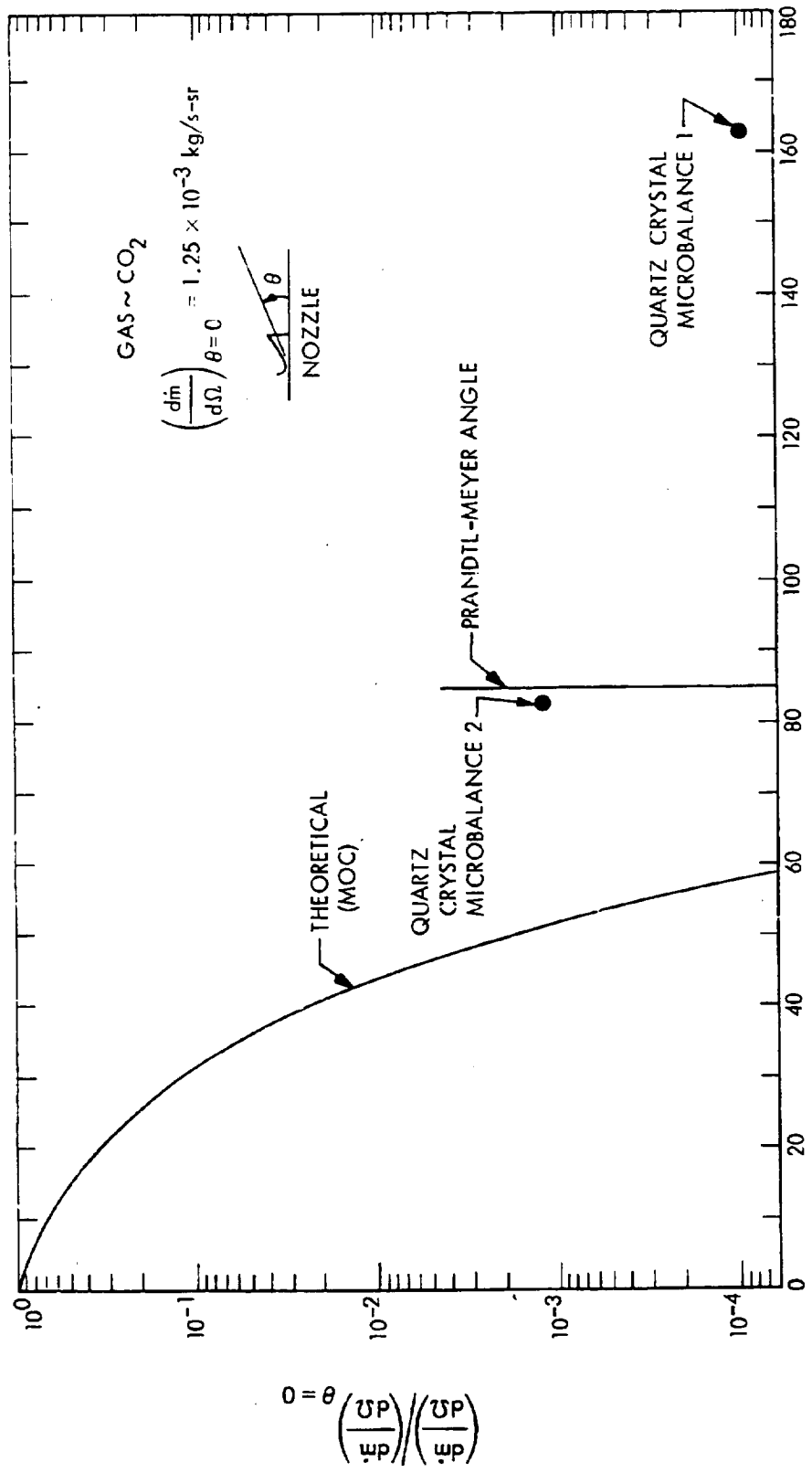

Fig. 12. Plume Boundary Data--CO_2

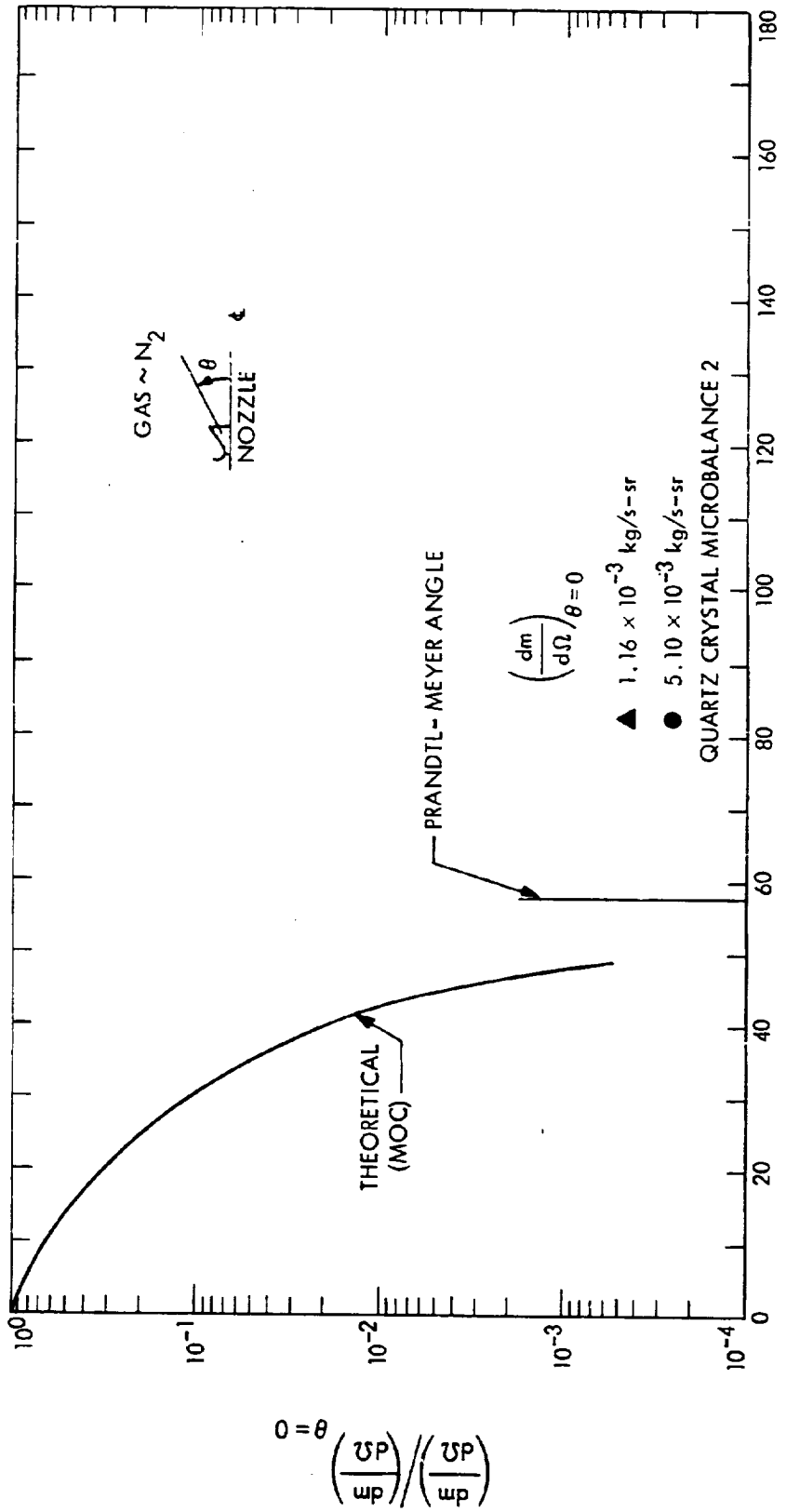

Fig. 13. Plume Boundary Data--N_2